A Reliable, Repetitively Pulsed, High-Power Nitrogen Laser*

Benjamin W. Woodward[†] and Vernon J. Ehlers[‡]
Joint Institute for Laboratory Astrophysics, [§] *University of Colorado, Boulder, Colorado 80302*

W. C. Lineberger[||]
Department of Chemistry and Joint Institute for Laboratory Astrophysics, University of Colorado, Boulder, Colorado 80302

(Received 12 February 1973; and in final form, 19 March 1973)

The design and construction of high-power nitrogen 3371 Å laser is described in detail. The laser produces 13 mJ at 3371 Å in a 12 nsec FWHM pulse at a repetition rate of 5 pulses per second. Various models of the laser have yielded 10^8 pulses with very infrequent component failure. When a second mirror is added, strong laser action is observed in the N_2 first positive system; the total resultant ir output energy is about 3 mJ in a 50 nsec FWHM pulse.

INTRODUCTION

In 1963 Heard obtained laser action in a fast nitrogen discharge.[1] He observed 30 lines in the ultraviolet, the strongest emission being near 3371 Å. This corresponds to the (0,0) transition from N_2 $C^3\Pi_u$ to N_2 $B^3\Pi_g$, the second positive system of N_2.

Because the laser employed an inexpensive, readily available gas, operated at room temperature, was easily constructed, and held promise of being a bright source of ultraviolet radiation, development proceeded very rapidly. In the decade since Heard's initial discovery, several different types of nitrogen lasers have been reported,[2–10] most of which fall into two broad classes: (1) low-power, (≤ 100 kW) reliable lasers, and (2) high-power single shot lasers. The highest power reported to date is approximately 2.5 MW in a 4 nsec pulse.

The ease with which dye lasers can be pumped by an N_2 laser made it clear that a repetitively pulsed, high-power nitrogen laser would be a very useful laboratory tool. The short spontaneous emission lifetime of the $C^3\Pi_u$ state, approximately 40 nsec, causes the major design problems for this application. In order to achieve population inversion and a high proportion of stimulated emission, one must populate this state in a time short compared to its lifetime. The electrical switching system described here deposits 25 J of energy in the discharge channel in about 50 nsec. This excitation quite easily provides output powers greater than 1 MW at repetition rates of 5 pulses per sec. We have not attempted to increase the repetition rate, although this should be a straightforward task, at least up to 50–100 pulses per sec.

Throughout the design and construction of the lasers we used components providing a high degree of reliability; the lasers reported here have operated for two years, yielding approximately 10^8 pulses. The only components needing replacement were several capacitors in the capacitor bank. In this paper we briefly discuss some theoretical aspects of the electrical design of a nitrogen laser, then deal with the practical aspects of both the electrical and mechanical designs.

I. ELECTRICAL DESIGN

The primary factor affecting the energy output of a nitrogen laser is the time scale for excitation of the nitrogen gas; i.e., the time required to transform the electrical energy stored in the capacitor into excitation energy of the gas. As a result, the electrical design of the exciting circuit is of major importance, while the mechanical design of the laser channel plays a secondary role.

A. Circuit Theory

The electrical energy is stored in a bank of capacitors; the prime design objective is to discharge this energy into the nitrogen gas as rapidly as possible. Because of the short time scale involved, a simple lumped-circuit analysis of the discharge circuit is inadequate. The cables between the capacitor and the laser must be included in the analysis as a pulse-forming transmission line. An additional complication arises because the laser is not represented by a fixed impedance; its equivalent resistance changes over many orders of magnitude during commutation. Consider the temporal behavior of the lumped-parameter equivalent circuit shown in Fig. 1. When the switch S is closed, the energy stored in C does not immediately appear across R_l, the laser. Rather, the pulse-forming line capacitance C_t first charges up and then transfers its energy to the gas. The significance of this fact was noted by Geller *et al.*,[11] who pointed out that the laser electrical-discharge conditions are somewhat independent of capacitor and switch inductances if the two-way transit time of the transmission line is larger than the excitation time in the gas. In this case, the rise time for the discharge in the laser is limited primarily by L_t and L_l. The laser output depends on the characteristics of the capacitor and switch only in that the laser breakdown voltage increases as the rate of voltage rise increases. Further, the impedance of the laser gas after breakdown has started is very small, so that the maximum coupling of power to the discharge will occur when the impedance of the transmission line is minimum (in the range available).

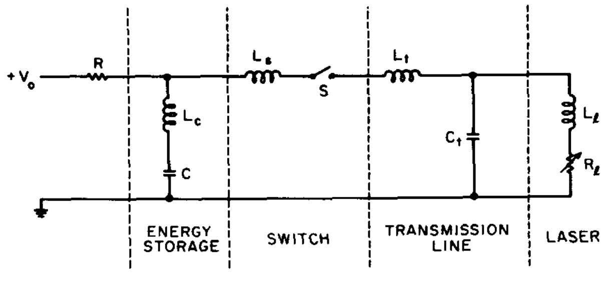

FIG. 1. The equivalent electrical circuit used in the lumped-circuit analysis of the pulsed nitrogen laser electrical system.

Geller and co-workers[11] show that laser power increases linearly with breakdown voltage, with the slope inversely proportional to the transmission line impedance. But because inductance and impedance are so closely related [$Z=(L/C)^{\frac{1}{2}}$ for a transmission line], one cannot be certain which is the controlling parameter without extensive testing.

We find, however, that the most important way to increase power in a nitrogen laser is to reduce the inductance and impedance of the transmission line. Since the inductance and impedance scale together with transmission line changes, we use the terms almost interchangeably here.

B. Circuit Design

The detailed circuit diagram for the laser discharge circuit is shown in Fig. 2. In Table I we list specific components used in this circuit for the three generations of lasers we have constructed; note that the three lasers differ substantially in scale. Basically, the circuit is very simple. The capacitor bank C_0 is charged by an external power supply V_0. A trigger pulse is amplified and applied to the grid of a large hydrogen thyratron T_0. The conduction of the thyratron effectively grounds the high-voltage side of capacitor bank C_0, resulting in the stored energy being transferred to the transmission line and thence to the laser.

When the large thyratron fires, a large, positive voltage spike appears on the grid and on the heater lines. Thus we have inserted a high-voltage diode, D_0, on the trigger line and have placed π filters in the heater circuit to provide protection for the small trigger thyratron and the heater transformers, respectively.

The first laser built used standard RG-8 cable for the transmission lines. In view of the importance of low-impedance transmission lines mentioned above, Belden YK-217 cable was used in the succeeding two models; this is a special high-voltage, low-impedance cable[12] designed for high-current, high-voltage pulses with nearly full reversal. Its capacitance is approximately 360 pF/m, its inductance is 95 nH/m, and its characteristic impedance about 17 Ω. The inductance was further minimized by providing many cables for transmitting electrical energy from the capacitor to the laser. Our experience with these transmission lines is in agreement with the qualitative theory outlined above. The laser output power is inversely related to the transmission-line inductance, while changes in circuit inductance near the switching element have little effect on laser output power. In Fig. 3 we show the laser output power plotted as a function of the reciprocal of the transmission line inductance.

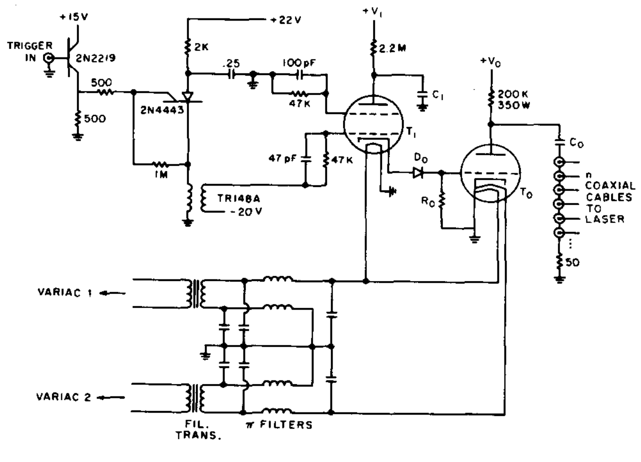

FIG. 2. Detailed circuit diagram of the electrical circuit used to produce the nitrogen laser discharge.

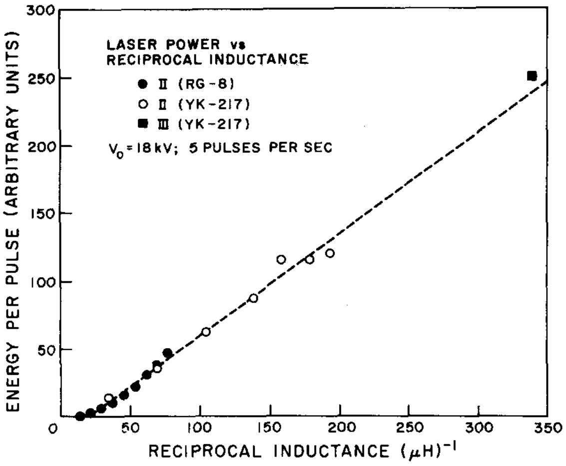

FIG. 3. The output power as a function of the inductance of the transmission lines. The majority of the points were obtained on the intermediate-size laser; the closed circles were obtained using RG-8 cable. The square point was obtained using the largest laser and YK-217 cable.

The large hydrogen thyratrons used in this circuit have distinct advantages over triggered spark gaps. The thyratrons can be triggered by a smaller voltage pulse, provide greater shot-to-shot stability, can be fired at much higher repetition rates, and, most important, have a much longer lifetime. Although we exceed the published peak-current and peak-power maximum ratings on these tubes by a wide margin in our system, no deleterious effects have been observed. The reason presumably lies in the fast switching time used here; our commutation time is less than 100 nsec, while the manufacturer's ratings refer to applications in which the commutation time is in the microsecond domain.

TABLE I. Elements for the nitrogen laser discharge circuit shown in Fig. 2.

Element	Specification I (Small laser)	II (Midsize laser)	III (Large laser)
Hydrogen thyratron EGG	HY-1A	1802	HY-5
Capacitor bank C_0 (Sprague ceramics)	10 nF, 30 kV	30 nF, 30 kV	50 nF, 40 kV
Grid resistor R_0	500 Ω	400 Ω	100 Ω
High voltage diode D_0	10 kV	10 kV	15 kV
Trigger tube T_1	2D21[a]	3C45	3C45 or larger
Voltage V_1	1 kV[a]	2 kV	3 kV
Capacitor C_1	500 pF[a]	500 pF	1000 pF
Transmission line	RG-8 (12 parallel cables)	YK-217 (29 parallel cables)	YK-217 (60 parallel cables)
V_0 (max)	20 kV	25 kV	37 kV
V_0 (typical)	18 kV	22 kV	30 kV
Energy per pulse at V_0 (typical)	0.5 mJ	3 mJ	12 mJ

[a] These elements have also been deleted in this size laser, with the trigger transformer driving the HY-1A directly.

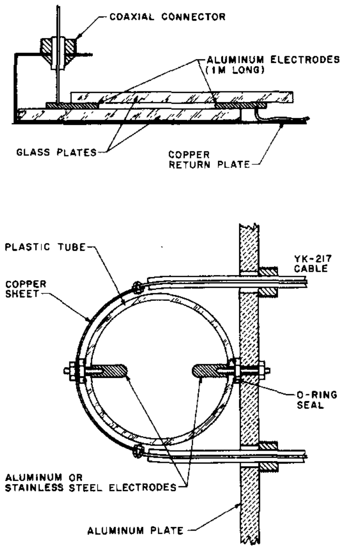

FIG. 4. (Upper) Cross sectional view of the narrow-channel flat nitrogen laser. (Lower) Cross sectional view of the round-channel nitrogen laser.

The laser output is insensitive to the type of trigger circuit used to fire the large hydrogen thyratron.

II. MECHANICAL DESIGN

A. Laser Section

We have experimented with two different geometries for the discharge tube. In one case we used a tube with a narrow, rectangular cross section; the other tube studied had a simple circular cross section. In both cases we used transverse-field excitation, as this offers a much faster voltage rise time than the longitudinal discharge used by some workers.

The flat channel geometry we studied is basically that due to Avco–Everett researchers[2]; the particular configuration we used is displayed in Fig. 4. The discharge is confined to a volume very near one or both side walls of the channel, depending on the location of the discharge current return line. This feature is advantageous in that the volume of excited molecules is well defined, but this advantage is partially offset because deviations from flatness in the wall surface may prevent a substantial fraction of the excited molecules from participating in stimulated emission. We have studied minimum-inductance configurations of this basic design, using both Plexiglas and glass as side wall materials. This design is useful if one wishes to operate the laser with a high repetition rate; the energy per pulse does not fall off as rapidly with increasing repetition rate as it does with the circular tube configuration. However, we obtain more energy per pulse when using the circular geometry.

The circular-tube discharge channel was originally developed by workers at EGG Nuclear.[13] In this configuration, shown at Fig. 4, the walls are far removed from the electrical discharge. The breakdown voltage is larger than in the narrow-channel design, leading to the higher peak output power mentioned above. Because our application requires maximum possible energy per pulse, we have concentrated on this particular configuration; the three models mentioned in Table I are all of this design. We also find the simplicity of this design to be advantageous. Different electrode shapes, materials, and separations can be tested quite readily as the electrodes are demountable. A modular design is used for the output window and mirror sections; these modules attach to the ends of the circular discharge tube and can be readily removed.

The mirror and window are held in place against O-ring seals by means of Plexiglas flanges. Both of these components can readily be aligned by tightening the flange screws appropriately and thus partially compressing the O ring. Viton O-rings are used for the vacuum seals, because Buna-N seals deteriorate very rapidly in the presence of ozone. The discharge tube itself is a simple Plexiglas tube with a 6.35 mm wall thickness.

B. Electrical Section

There are many conflicting design considerations for the capacitor–thyratron housing. The capacitor bank is charged to 30–40 kV, and thus adequate electrical insulation must be provided. At the same time, the thyratron runs at a high temperature and consequently the insulation must be able to sustain these elevated temperatures. Furthermore, the capacitor should be thermally isolated from the thyratron heat source. Another consideration arises because the peak current is tens of kiloamperes; thus the resistance must be small and the inductance should be minimized to improve the voltage-pulse risetime. Finally, the entire structure must have sufficient mechanical strength to support a large number of coaxial cables.

The mechanical design of the switching circuit design is shown in Fig. 5. Aluminum cylinders with O-ring-sealed flanges are employed to house the capacitor and the thyratron. A glass insulator is placed around the thyratron and a Plexiglas insulator around the capacitor bank; a silicon-rubber cement is used to join the two insulators. A low-inductance, low-thermal-conductivity, thin-walled cylinder electrically connects the thyratron to the capacitor while minimizing heat transfer. Further cooling is provided by

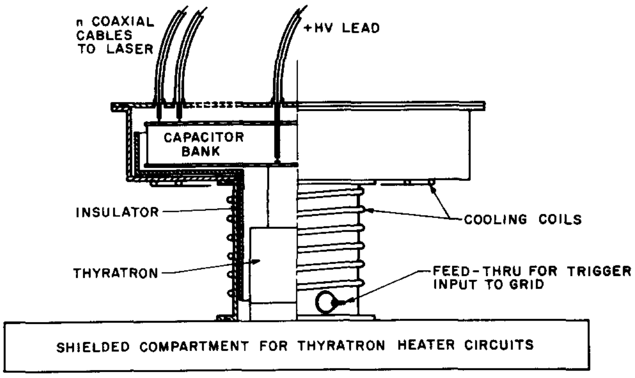

FIG. 5. Mechanical design of the housing for the capacitor bank and thyratron.

water cooling the aluminum housing for the capacitor bank. The entire housing is filled with SF_6 to reduce corona discharge. The coaxial cables are connected to the top plate of the capacitor housing, and the inner conductors of the cables pass through the aluminum plate and make contact with the top plate of the capacitor bank.

A large number of coaxial cables are used to connect the capacitor bank to the laser electrodes in order to minimize transmission-line impedance. At the laser tube, the coaxial cables are connected at equal intervals to a broad copper sheet, which in turn is connected to one laser electrode along its entire length. The other laser electrode is attached to a thick metal slab; this slab not only provides the electrical return path, but is also the primary mechanical support for the laser tube (see Fig. 4).

III. PERFORMANCE

All three of the lasers described above have been used extensively as tools in experimental work. In this section we analyze their performance, discussing it primarily in terms of the largest laser. In addition, based on more than 3 yr operating experience, component reliability is evaluated.

A. Laser Output

The principal output of the pulsed molecular nitrogen laser is an envelope of spectral lines centered at 3371 Å and less than 1 Å wide. A spectrum obtained from the small laser is shown in Fig. 6; this spectrum is typical of all three versions. The output pulse from the smaller two lasers is approximately 10 nsec in duration and has a shape which is roughly a skewed Gaussian. We found, however, that the pulse shape from the largest laser is more nearly triangular with a 12 nsec full width at half-maximum.

The power measurements displayed in this paper were obtained using a large-area Scientech 3600 power meter. What is actually measured is the time average of the total energy absorbed by the thermopile. The pulse power quoted is the approximate peak power given by

$$P=\frac{E}{\Delta t}=\frac{\text{energy per pulse}}{\text{pulse FWHM}}.$$

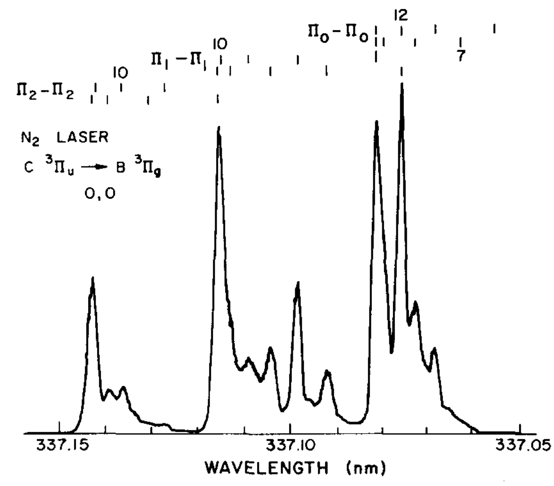

FIG. 6. The output spectrum obtained from the smallest round-channel nitrogen laser.

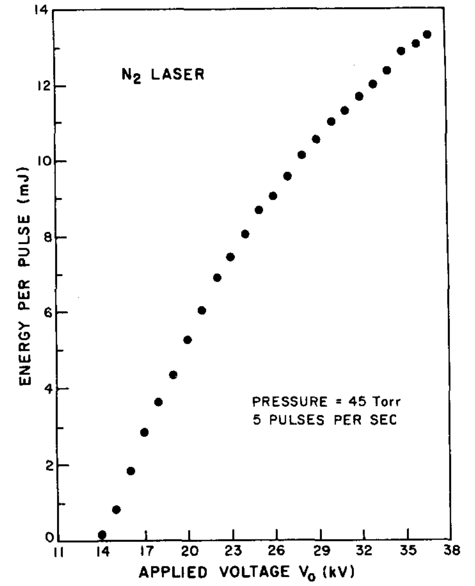

FIG. 7. The output power of the nitrogen laser as a function of the voltage applied to the capacitor bank.

With a given electrical and mechanical configuration, the output power depends only on the charge stored in the capacitor and on the energy distribution of electrons in the plasma. The cross section for the direct electron excitation of the $C^3\Pi_u$ state rises sharply from threshold at 11.05 eV to a peak at about 15 eV and then falls off slowly at higher electron energies. With a Maxwellian distribution of electron energies the mean energy is proportional to E/p, and one would expect a rather broad maximum in C-state excitation as a function of applied electric fields. Under the nonequilibrium conditions present in the discharge, the precise electron energy distribution is unknown. The relative laser output power as a function of capacitor-bank voltage is shown in Fig. 7. The output power as a function of nitrogen pressure at a number of different voltages is shown in Fig. 8. Reducing the length of the active discharge by a factor of 2 while keeping pressure, input voltage, and energy constant does not significantly affect the output power.

The output energy per pulse and the total energy output as a function of repetition rate are displayed in Fig. 9. Note that the output-per-pulse peaks at a repetition rate of approximately 4 pulses per sec. It appears that preionization plays some role in achieving an efficient discharge, and that the lower output at repetition rates below 4 pulses per sec arises because the ions present either recombine or are swept away from the electrode region before the next pulse. The decrease in energy per pulse above 4 pulses per sec arises because at higher repetition rates the N_2 gas is not replaced between discharges. This has two effects: presence of metastable species in unusable electronic configurations, such as dissociated atoms and electronically excited molecules, and presence of rotationally or vibrationally hot molecules for which electron excitation to appropriate ex-

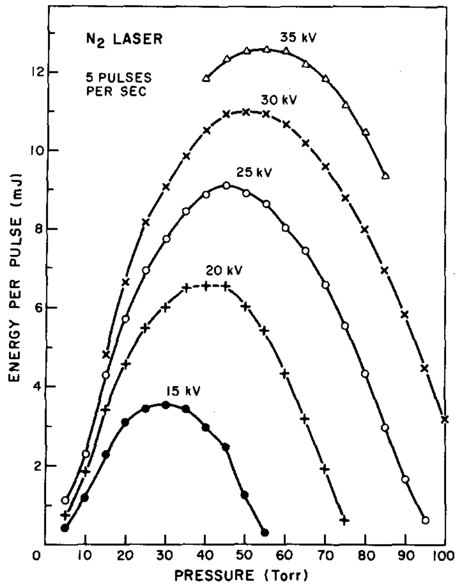

FIG. 8. The output power of the nitrogen laser as a function of the nitrogen pressure, measured at various applied voltages.

TABLE II. Nitrogen laser performance.

Source	Pulse width (FWHM) (nsec)	Maximum peak power (kW)	Typical pulse repetition rate (Hz)	Maximum average power (mW)
Svedberg, Högberg, and Nilsson[7]	0.6	0.002	···	···
Ericsson and Lidholt[6]	0.7	1–2	200	0.1–0.3
Phillips and West[8]	6	1	120	0.7
Dreyfus and Hodgson[9]	2, 7	60	···	···
Shipman[5]	4	2500	single shot	···
Avco-Everett Research Laboratory—model C 5000	10	100	500	500
Molectron Corp. model VV-200	10	250	15	30
This work I	10	50	20[a]	10
II	10	300	20[a]	60
III	12	1100	10[a]	130

[a] These repetition rates are not maximum, but are the values for which the energy per pulse is 70–80% of its maximum value (see Fig. 9).

cited states is unlikely. In support of this conjecture we note that the Lewis–Rayleigh afterglow can be easily observed after the main discharge; furthermore, we calculate that a reasonably large fraction of the molecules end up in the $A^3\Sigma_u$ metastable states with radiative lifetimes in the range 1–2 sec. The effectiveness of collisions in quenching the metastable molecules is of considerable importance in determining the nitrogen state distribution at the onset of the next pulse. It is apparent that thermal equilibrium is difficult to achieve in less than 0.1 sec since 20 J dissipated in 10^{19} molecules corresponds to 12 eV per molecule. It is clear that the walls and electrodes must play an important role in removing energy from the system. A random walk estimation shows that it takes some tens of milliseconds for a molecule in the center of this discharge to reach a surface. In a flat-channel laser the time to reach a surface is considerably less; this explains the superior performance of the flat laser at high repetition rates.

In order to test the hypothesis that the repetition rate limitation is due to an undesirable distribution of states in the nitrogen molecules, helium was added to the discharge to speed thermal cooling. At a repetition rate of 5 per sec the helium made no measureable difference, but as the repetition rate increased the helium had a greater effect. At 20 pulses per sec the laser output power increased 15% when approximately 40 Torr of helium was added to the system. Another test was performed by measuring the output power as a function of the nitrogen flow rate. The output power increased as the nitrogen flow rate increased, reaching its optimum level at a flow rate of approximately 300 atm liter/sec. At this flow rate most of the metastable molecules are apparently swept out of the region between the electrodes between laser pulses.

These data support the idea that the molecular state distribution is altered by the discharge and that an undesirable distribution persists for as long as 100–200 msec. It is evident that nearby surfaces, a suitable buffer gas, and rapid gas flow can play important roles in returning the molecular nitrogen to its normal distribution. The decrease in total power output above 40 pulses per sec is caused by the long time constant of the charging circuit; above this frequency the capacitor bank does not charge up to its full voltage before the thyratron fires.

In addition to the nitrogen-molecule ultraviolet laser lines at 3371 Å, other radiation is also present. We have observed laser action of the infrared lines in the first positive band.[10,14] Because the lifetime of the inverted levels in this case is longer than for the second positive band, the output power for these infrared lines is more dependent upon the Q of the optical cavity. When an 8%-reflectivity output mirror is added to the system, the infrared power becomes substantial. For example, the large laser typically delivers 3 mJ per pulse on the infrared lines; this is 20% of the total output energy, and represents the highest power in the first positive system reported to date.

Table II contains a summary of the performance of the nitrogen lasers described in this paper and a comparison with other lasers described in the literature or commercially

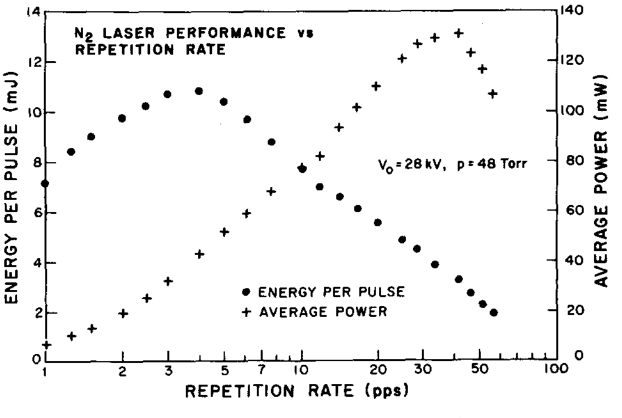

FIG. 9. The output energy per pulse and the total output energy per second (average power) as a function of the repetition rate of the nitrogen laser.

available. Note that the comparison may be misleading, for some of the low-power designs have features such as low beam divergence, simplicity of design, or high repetition rates which make them desirable for certain applications.

B. Reliability

An important requirement of a research instrument is that it be a dependable tool. In our applications, a great many shots are required; the intermediate laser has delivered 10^8 shots and the larger laser has delivered more than 10^7 pulses. This extensive operation has provided a good opportunity to evaluate the reliability of the various laser components.

Up to this point we have had only one thyratron failure; an EGG 1802 thyratron failed to withstand the high voltage after 5×10^7 shots. The plastic laser tubes developed numerous internal cracks, but shattered in only one case. Aluminum or stainless steel appear to be the best electrode materials; brass electrodes tend to become pitted after 10^7 discharges.

By far the most frequent failures occur in the capacitors used in the capacitor bank. These are high-voltage capacitors of the type normally used in color television sets, and apparently are not manufactured to withstand the frequent charging and discharging to which they are subject in our apparatus. In a few cases the capacitor insulation has cracked; in still fewer cases the capacitor has shattered. Most capacitor failure, however, manifests itself as decreased capacitance. One particular batch of capacitors was extremely poor; after approximately 10^7 shots their capacitance had severely dropped, occasionally to as low as 15% of its specified value. However, such severe degradation was rare. In most cases capacitance had dropped by only about 10% after 10^7 shots.

C. Other Gases

It is clear that this laser can be used to search for laser action in any gas, although its major usefulness would be only in those cases where the inverted level possesses a short lifetime. In searching for laser action in neon, we have observed the 5401-Å line previously reported by Leonard and co-workers.[15,16] Output powers in excess of 25 kW were obtained for this line, with a pulse length of approximately 5 nsec. Although laser action in neon is interesting, we find it to be of limited usefulness. By using our large nitrogen laser to pump a tunable dye laser, we can obtain greater power in the green region than we can obtain using neon in the gas laser. Furthermore, the dye laser has the advantage of being tunable and avoids the expense of using neon, although it does have a longer pulse length. We have also introduced hydrogen into our laser and have searched for lasing action[17] in the vacuum ultraviolet. Considerable amounts of vacuum ultraviolet radiation have been observed, along with some slight indication that the system was lasing. This aspect has not been pursued.

---

[*] This research was supported by the Advanced Research Projects Agency of the Department of Defense, and was monitored by U. S. Army Research Office-Durham under Contract no. DAHC04 72 C 0047.

[†] Present address: National Bureau of Standards, Boulder, Colorado 80302.

[‡] National Science Foundation Science Faculty Fellow and JILA Visiting Fellow. Permanent address: Calvin College, Grand Rapids, Michigan 49506.

[§] Of the National Bureau of Standards and the University of Colorado.

[‖] Alfred P. Sloan Foundation Fellow, 1972–1974.

[1] H. G. Heard, Nature (Lond.) **200**, 667 (1963).

[2] D. A. Leonard, Appl. Phys. Lett. **7**, 4 (1965); E. T. Gerry, Appl. Phys. Lett. **7**, 6 (1965).

[3] J. Wilson, Appl. Phys. Lett. **8**, 159 (1966).

[4] M. Geller, D. E. Altman, and T. A. DeTemple, J. Appl. Phys. **39**, 3639 (1966).

[5] J. D. Shipman, Jr., Appl. Phys. Lett. **10**, 3 (1967); J. D. Shipman and A. C. Kolb, IEEE J. Quantum Electron. **QE-2**, 298 (1966).

[6] K. G. Ericsson and L. R. Lidholt, Appl. Opt. **7**, 211 (1968); Ark. Fys. **37**, 557 (1968).

[7] A. Svedberg, L. Högberg, and R. Nilsson, Appl. Phys. Lett. **12**, 102 (1968).

[8] D. T. Phillips and J. West, Am. J. Phys. **38**, 655 (1970).

[9] R. W. Dreyfus and R. T. Hodgson, Appl. Phys. Lett. **20**, 195 (1972).

[10] V. M. Kaslin, I. N. Knyazev, and G. G. Petrash, Sov. J. Quantum Electron. **1**, 466 (1972).

[11] M. Geller, D. E. Altman, and T. A. DeTemple, Appl. Opt. **7**, 2232 (1968).

[12] Available from Belden Corp.

[13] T. W. Nybakken (private communication).

[14] L. E. S. Mathias and J. T. Parker, Appl. Phys. Lett. **3**, 16 (1963).

[15] D. A. Leonard, IEEE J. Quantum Electron. **QE-3**, 133 (1967).

[16] D. A. Leonard, R. A. Neal, and E. T. Gerry, Appl. Phys. Lett. **7**, 175 (1965).

[17] R. T. Hodgson and R. W. Dreyfus, Phys. Rev. Lett. **28**, 536 (1972).